DYNAMIC ANALYSIS OF VARIABLE STRUCTURE FORCE CONTROL OF HYDRAULIC ACTUATORS VIA THE REACHING LAW APPROACH [1]

Mohammed Jerouane [*] **Nariman Sepehri** [**]
Françoise Lamnabhi-Lagarrigue [*]

[*] *Laboratoire des Signaux et Systèmes*
C.N.R.S - Supélec
91190 Gif-Sur-Yvette, France
[**] *Departement of Mechanical and Industrial Engineering*
The University of Manitoba,
Winnipeg Manitoba, R3T 5V6, Canada

Abstract: This paper describes the design and experimental analysis of a Variable Structure Control (VSC) law using three reaching law strategies for a hydraulic servo control system. For this purpose we use a nonlinear mathematical model to develop a stable variable structure force control. The controller is designed using a sliding mode equivalence control and is augmented by reaching law approach to further improve the performance. Three reaching laws are developed to bring the system states to the sliding mode surface. The feasibility of each reaching law structure on the closed loop performance (i.e, reaching time, chattering and quality of tracking) are experimentally evaluated and analyzed.

Keywords: Sliding mode, hydraulic actuator, dynamic analysis, , experiments.

1. INTRODUCTION

Hydraulic servo systems are widely used in various industrial applications such as hydraulic manipulators, precision machine tools and simulators. Hydraulic actuators are potential choices for modern industries due to their high force to weight ratio, fast response time and compact size. However, hydraulic systems are complex and pose nonlinearities. Control volume changes, frictions and orifice area openings cause nonlinearities while uncertainties stem from fluctuation in the supply pump pressure, changes in the environmental stiffness, load fluctuation, oil compressibility and many more.

Force control in hydraulic actuators is particularly a difficult problem. PID controllers do not yield a reasonable performance for the wide range of operating conditions (Alleyne *et al.*, n.d.), (Niksefat and Sepehri, 1999). Given the limitations of fixed-gain controllers, several researchers considered the use of adaptive controllers. Most of the adaptive controllers that have been developed, including the ones by Huang and Wang (Huang *et al.*, 1994), Kotzev et al. (Kotzev *et al.*, 1994), Bobrow and Lum (Bobrow and Lum, 1995) are based on the linearization of nonlinear dynamics around either the equilibrium or the desired set-point. As a result, the lack of a global stability proof is often a disadvantage.

Nonlinear dynamics of a hydraulic actuators have been considered to formulate nonlinear control

[1] The authors wish to acknowledge the support of the Natural Sciences and Engineering Research Council (NSERC) of Canada

laws. Sohl and Bobrow (Sohl and Bobrow, 1999) applied a Lyapunov technique to design a nonlinear control law for hydraulic servo systems. The controller provided excellent force and position tracking capabilities, but many practical factors such as changes in the load, supply pressure and flow gain were not explicitly considered. They also used the derivatives of the desired force, which in turn involves the piston acceleration. Hence, either differentiation of measured piston velocity, or an accelerometer sensor is required. Niksefat and Sepehri (Niksefat and Sepehri, 2000) presented an explicit force controller for a hydraulic actuator based on a nonlinear version of Quantitative Feedback Theory. The results showed that the compensated system is not sensitive to the variation of parameters such as environmental stiffness or supply pressure.

Variable Structure Control (VSC) has been studied as an alternative control law for a hydraulic servo system (**?**), (Huang *et al.*, 1994), (Lee and Lee, 1990). It appears that most VSC laws require the differentiability of the arbitrary load or resistive torques (Huang *et al.*, 1994), or the use of the derivatives of piston velocity (**?**), (Jerouane and Lamnabhi-Lagarrigue, 2001), which is difficult to obtain. In addition, little attention has been given to the dynamic characteristics of the reaching laws. A VSC with sliding mode techniques is built on mainly two steps: proper choice of sliding surface and the choice of reaching law (sliding reachability) which enforces the closed loop trajectory to reach the manifold asymptotically. However, such an approach does not exclude the possibility of using other functions to achieve similar purposes (Gao and Hung, 1993). The reaching law approach has been proposed by Gao et al. (Gao and Hung, 1993) on 1993. The method simultaneously takes care of ensuring the reaching condition, influencing the dynamic quality of the system during the reaching phase, and providing the means for controlling the chattering level.

In this paper we present the design and experimental evaluation of a variable structure control law for an electro hydraulic servo force control system using three reaching law strategies. It is our goal to accomplish these objectives:

(1) Design of a nonlinear VSC force controller for an hydraulic system. The controller should exhibit a good transient behavior (i.e., fast response with acceptable overshoot) and small steady-state error without requiring acceleration feedback or derivatives of cylinder chamber pressures.
(2) Investigate the effect of three reaching laws on the system's performance, specially the closed-loop performance, i.e., reaching time, chattering and quality of regulation.
(3) Experimental validation of the findings.

This paper is organized as follows. Section 2 describes the test rig and the modelling of the hydraulic system. Section 3 presents the design of variable structure control law including the design of the equilibrium manifold, and the control selection using various reaching law methods to drive the state plant trajectory on this equilibrium. Section 4 presents experimental results and analyze the effect of the various reaching law structures on the system performances. Finally, conclusions are provided in Section 5.

2. DESCRIPTION OF THE TEST RIG

The experiment setup, on which all experiments were carried out, is shown in Fig. 1. The system is powered by a motor-driven hydraulic pump with pressure up to $2650psi$. The actuator is connected to and controlled by a Moog 765 two-stage servovalve. The valve is controlled by a PC equipped with a data acquisition board and an encoder card. The displacement of the actuator is acquired using a quadrature incremental encoder. Transducers mounted on the hydraulic circuit transmits various pressures to the data acquisition board, the board transmits control signals generated by PC to the valve servo.

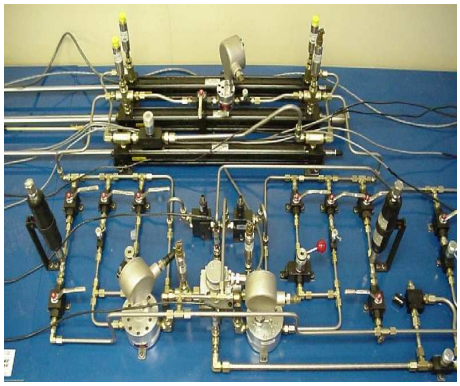

Fig. 1. The experiment setup of hydraulic system

The dynamic of the valve servo in its simple can be given as

$$u = (\frac{\tau}{k_{sp}})\frac{dx_{sp}}{dt} + \frac{1}{k_{sp}}x_{sp} \quad (1)$$

where x_{sp} is the valve spool displacement, u is the input signal, τ is the time constant, and k_{sp} is the servo valve gain.

In this work, we assume that the control input u is proportional to the spool displacement, x_{sp} (i.e., $x_{sp} = k_{sp}u$). This choice is motivated by the fact that the servo valve response is much faster than the rest of hydraulic servo system. Thus the servo valve dynamics can be simplified even further without loss of generality.

The piston motion is obtained by modulating the oil into and out of the cylinder chambers, which are connected to the servo valve through cylinder ports. The piston controls the flow of the hydraulic fluid into and out of the actuators. The flow rates

(q_i, q_o) are expressed as
$x_{sp} > 0$ $(extension)$

$$q_i = C_d w x_{sp}\sqrt{\frac{2}{\rho}}\sqrt{(p_s - p_i)}, q_o = C_d w x_{sp}\sqrt{\frac{2}{\rho}}\sqrt{(p_o - p_e)} \quad (2)$$

$x_{sp} \leq 0$ $(retraction)$

$$q_i = C_d w x_{sp}\sqrt{\frac{2}{\rho}}\sqrt{(p_i - p_e)}, q_o = C_d w x_{sp}\sqrt{\frac{2}{\rho}}\sqrt{(p_s - p_o)} \quad (3)$$

where q_i and q_o are the fluid flows into and out of the valve, respectively. C_d is the orifice coefficient of discharge, ρ is the mass density of the fluid, p_s is the pump pressure, p_e is the return pressure, and w is the area gradient that relates the spool displacement, x_{sp}, to the orifice area.
The differential equation for the cylinder pressures, P_i and P_o, can be written as (Niksefat and Sepehri, 2000)

$$\frac{dP_i}{dt} = \frac{\beta}{V_i}(q_i - A_i\frac{dx}{dt}) \quad (4)$$

$$\frac{dP_o}{dt} = \frac{\beta}{V_o}(-q_o + A_o\frac{dx}{dt}) \quad (5)$$

where x is the piston position, β is the effective bulk modulus of the hydraulic fluid and, V_i and V_o are initial volumes of the cylinder chambers. $A_j (j = i, o)$ are piston areas.
The dynamic motion of the piston is described by

$$m_a\ddot{x} = (A_i P_i - A_o P_o) - d\dot{x} - k_e(x - x_e) \quad (6)$$

where m_a is the total mass of piston, rod and load, d is the viscous damping coefficient, and x_e is the location of the environment. The environment is represented by a pure stiffness k_e. The system parameters are given in Table 1.

Table 1: Physical parameters of the hydraulic system.

System parameter	*Symbol*	*Nominal Value*
servo valve spool position gain	k_{sp}	$12(10)^{-05}[m/Kg]$
servo valve time constant	τ	$35[ms]$
total mass of piston rod and load	m_a	$12[Kg]$
viscous damping coefficient	d	$1000[Ns/m]$
servo valve coefficient of discharge	C_d	0.61
servo valve orifice area gradient	w	$2.75(10)^{-02}[m]$
piston areas	A_i, A_o	$6.33(10)^{-04}[m^2]$
initial volume of each chamber	V_i, V_o	$0.33(10)^{-04}[m^3]$
effective bulk modulus	β	$689MPa[kg/m^3]$
hydraulic fluid density	ρ	$847[kg/m^3]$
load spring constant	k_e	$75[KN/m]$

3. CONTROLLER DESIGN

The controller design is based on the nonlinear model presented in the previous section. The control algorithm is derived using a sliding mode equivalence control and is complemented by reaching law methods for driving the system to this manifold and maintaining there.

3.1 Control Problem

Let $F = A_i P_i - A_o P_o$ be the net force applied on the piston, F_d be the desired force, and $\boldsymbol{x} = \{x, \dot{x}, F\}^T$ be the state vector. Given the hydraulic system described by the nonlinear model, we observe that with respect to the desired force, the equilibrium state of this system is defined as

$$\boldsymbol{x}_{equilibrium} = \{x_d, 0, F_d\}^T \quad (7)$$

where x_d is the solution of equation (6) for $F = F_d$, from the following relation

$$m_a\ddot{x}_d = F_d - d\dot{x}_d - k_e x_d \quad (8)$$

The control problem is to find a nonlinear sliding mode controller that asymptotically stabilizes the equilibrium point (7).

3.2 Controller Design

The development of the VSC scheme for stabilization of the hydraulic system consist of two phases. The first phase is the design of an equilibrium manifold where the hydraulic system exhibits the desired properties in the presence of external disturbances and/or model uncertainties. The second phase is to design a scheme to drive the system to the equilibrium manifold and maintain it there.
The design of the sliding surface is done as follows. Consider the following sliding surface:

$$\sigma(\boldsymbol{x}) = F - F_d \quad (9)$$

where $F = A_i P_i - A_o P_o$ is the hydraulic force and F_d is the desired force.
Controller design is the second phase of the VSC design procedure. From equations (4) and (5), the derivatives of the active force is given by

$$\begin{aligned}\dot{F} &= \frac{d}{dt}(A_i P_i - A_o P_o) \\ &= A_i[\frac{\beta}{V_i}(q_i - A_i\dot{x})] - A_o[\frac{\beta}{V_o}(-q_o + A_o\dot{x})]\end{aligned} \quad (10)$$

Assuming small piston displacements, the following approximation is made

$$\frac{V_i}{\beta} \approx \frac{V_o}{\beta} = C \quad (11)$$

Equation (10) yields

$$\dot{F} = \frac{1}{C}\{A_i[(q_i - A_i\dot{x})] - A_o[(-q_o + A_o\dot{x})]\} \quad (12)$$

Using the derivatives of the active force from equation (12), the sliding mode equation becomes

$$\begin{aligned}\dot{\sigma}(\boldsymbol{x}) &= \dot{F} - \dot{F}_d \\ &= \frac{1}{C}\{A_i[(q_i - A_i\dot{x})] - A_o[(-q_o + A_o\dot{x})]\} - \dot{F}_d\end{aligned} \quad (13)$$

It is known that the transient dynamics of a VSC system consists of tow modes - a *reaching mode* or *nonsliding mode*, and a *sliding mode* (Gao and Hung, 1993). The dynamics of the equilibrium manifold (13) will be specified successively by three reaching law structures: the constant

rate reaching law, the constant plus proportional rate reaching law, and the power rate reaching law. Next, we define the class of popularly used reachability conditions and present analytical expressions of three reaching laws used through this paper.

3.3 Reaching law method for VSC Design

A broad class of popularly used reachability conditions can be considered as special cases of the following definition.

Definition 1. A sliding reachability condition is defined as

$$\dot{\sigma}(\boldsymbol{x}) = -\gamma(\sigma) \tag{14}$$

where $\gamma(\sigma)$ satisfies the following two conditions:

(1) $\gamma(\sigma)$ is continuous if $\sigma \neq 0$, and
(2) equation (14) is asymptotically stable.

This definition is based on the stability consideration of the $\sigma - dynamics$ (14). In fact, if one choose a radially Lyapunov function candidate $V(\sigma) = \frac{1}{2}\sigma^T\sigma$. The derivative of $V(\sigma)$ along the trajectory of (14) is

$$\dot{V}(\sigma) = -(\sigma)^T\gamma(\sigma)$$

which is negative and thus guarantees that the σ-dynamics is globally asymptotically stable.
In this work, we consider three reaching law as described by Gao el al. (Gao and Hung, 1993). Given an initial condition $\sigma(t_0)$, the reaching laws, $\dot{\sigma}(\boldsymbol{x})$, and their reaching time, T_r, are given below:

(1) ***Constant reaching law***

$$\gamma(\sigma, K_\sigma) = K_\sigma sgn(\sigma(\boldsymbol{x})), \quad K_\sigma > 0 \tag{15}$$

$$T_r = \frac{\sigma(t_0)}{K_\sigma} \tag{16}$$

(2) ***Constant plus proportional reaching law***

$$\gamma(\sigma, K_\sigma, K_p) = K_\sigma sgn(\sigma(\boldsymbol{x})) + K_p\sigma(\boldsymbol{x}), \quad K_\sigma, K_p > 0 \tag{17}$$

$$T_r = \frac{1}{K_p} Ln(\frac{K_\sigma + K_p|\sigma(t_0)|}{K_\sigma}) \tag{18}$$

(3) ***Power reaching law***

$$\gamma(\sigma, K_\sigma, \alpha) = K_\sigma|(\sigma(\boldsymbol{x}))|^\alpha sgn(\sigma(\boldsymbol{x})), \quad K_\sigma > 0, \quad \alpha \in (0,1) \tag{19}$$

$$T_r = \frac{1}{K_\sigma(1-\alpha)}(\sigma_0)^{(1-\alpha)} \tag{20}$$

For the three reaching law described above, the dynamics of the equilibrium manifold are described as

$$\begin{aligned}\dot{\sigma}(\boldsymbol{x}) &= \mathbf{R}(\boldsymbol{x}) \\ &= \begin{cases} -K_\sigma sgn(\sigma(\boldsymbol{x})) \\ -K_\sigma sgn(\sigma(\boldsymbol{x})) - K_p\sigma(\boldsymbol{x}) \\ -K_\sigma|(\sigma(\boldsymbol{x}))|^\alpha sgn(\sigma(\boldsymbol{x})) \end{cases}\end{aligned} \tag{21}$$

Proposition 2. Given the nonlinear model of the hydraulic system (i.e., equations (1) to (6), and the sliding surface defined by equation (9) with a reaching law structure $\mathbf{R(x)}$. Then, the following variable structure control law

$$u = \frac{1}{k_{sp}\xi}[(A_i^2 + A_o^2)\dot{x} + \mathbf{R}(\boldsymbol{x})] \tag{22}$$

where

$$\xi = \begin{cases} A_iC_dw\sqrt{\frac{2}{\rho}}\sqrt{(p_s - p_i)} + A_oC_dw\sqrt{\frac{2}{\rho}}\sqrt{(p_2 - p_r)} & x_{sp} \geq 0, \\ A_iC_dw\sqrt{\frac{2}{\rho}}\sqrt{(p_i - p_r)} + A_oC_dw\sqrt{\frac{2}{\rho}}\sqrt{(p_s - p_2)} & x_{sp} < 0 \end{cases}$$

ensures that the sliding motion exists on $\sigma(x)$ and the equilibrium point $\{x_p, \dot{x}_p, F\}^T = \{x_d, \dot{x}_d, F_d\}^T$ is asymptotically stable.

Proof 3. Sliding mode exist if

$$\sigma(\boldsymbol{x})\dot{\sigma}(\boldsymbol{x}) \leq 0$$

From equations (12), the derivatives of the actuator force is given by

$$\dot{F} = \frac{1}{C}\{A_i[(q_i - A_i\dot{x})] - A_o[(-q_o + A_o\dot{x})]\} \tag{23}$$

From equation (13), sliding mode condition is expressed as

$$\begin{aligned}\dot{\sigma}(\boldsymbol{x}) &= \dot{F} - \dot{F}_d \\ &= \frac{1}{C}\{A_i[(q_i - A_i\dot{x})] - A_o[(-q_o + A_o\dot{x})]\} - \dot{F}_d\end{aligned}$$

where F_d is a constant, q_i, q_o is given by equation (2, 3) and u is given by equation (22), yields (after some calculations)

$$\sigma(\boldsymbol{x})\dot{\sigma}(\boldsymbol{x}) = \frac{1}{C}\sigma(\boldsymbol{x})[\mathbf{R}(\boldsymbol{x})]$$

We now replace the term , $\mathbf{R}(\boldsymbol{x})$, by its value given by equation (21), given

$$\begin{aligned}\sigma(\boldsymbol{x})\dot{\sigma}(\boldsymbol{x}) &= \frac{1}{C}\sigma(\boldsymbol{x})[\mathbf{R}(\boldsymbol{x})] \\ &= \begin{cases} \frac{1}{C}\sigma(\boldsymbol{x})[-K_\sigma sgn(\sigma(\boldsymbol{x}))] \\ \frac{1}{C}\sigma(\boldsymbol{x})[-K_\sigma sgn(\sigma(\boldsymbol{x})) - K_p\sigma(\boldsymbol{x})] \\ \frac{1}{C}\sigma(\boldsymbol{x})[-K_\sigma|(\sigma(\boldsymbol{x}))|^\alpha sgn(\sigma(\boldsymbol{x}))], \quad (0 < \alpha < 1) \end{cases}\end{aligned} \tag{24}$$

By choosing K_σ and K_p as positive constants, the reaching condition is obtained and the sliding mode occur on $\sigma(x) = 0$.

3.4 Experimental Results

The central objective of the design is to demonstrate the effectiveness of the proposed controller, to compare the capabilities of different reaching law structures, and to observe their effectivness on the closed-loop performances. Experimental study were conducted using the VSC law (22). The controller were implemented on the experimental test

stand shown in Fig. 1. All the experiments started at time $5s$ with a reference force $F_{ref} = 1000N$. The sampling frequency for the controller was $3ms$.
The controller parameters (K_σ, K_p and α) were selected such that:

(1) the controller provides a fast reaching (response) time ($Tr \approx 0.5sec$),
(2) the controller provides an acceptable overshoot ($d < 10\%$), and
(3) the controller ensures a small steady state error ($e_{ss} < 10N$) without chattering.

Property (3) is closely related to the steady-state performance while the rest are mainly related to the transient response.

3.4.1. Constant Reaching Law Fig. 2 shows experimental results of VSC law using constant reaching law strategy ($u = \frac{1}{k_{sp}\xi}[(A_i^2 + A_o^2)\dot{x} + K_\sigma sign(\sigma(x))]$). In this figure, the response of the hydraulic force F and the equilibrium manifold $\sigma(\boldsymbol{x})$ are given for three values of gain K_σ. When K_σ increases, the reaching time becomes small, but the chattering is high due to the high gain. The controller exhibits acceptable regulating capabilities and fast reaching time for high gain, but chattering occurs near the equilibrium manifold. On the other hand, the low gain controller $K_\sigma = 4 \times 10^{-08}$ makes the reaching time too long ($T_r = 1.2sec$) with a steady state error ($e_{ss} = 10N$) because of the non-reaching of the equilibrium manifold.
Using $K_\sigma = 5\times10^{-08}$, Fig. 3 shows the response of the hydraulic force (F), the discontinuous part of the control ($u_n = -K_\sigma sign(\sigma(\mathbf{x}))$), the continuous one ($u_c = ((A_i^2 + A_o^2)\dot{x})$), and the total control input (u). We see that the total control input, affected by the discontinuous part, is oscillatory and produces slight high frequency oscillations observed near the equilibrium manifold.

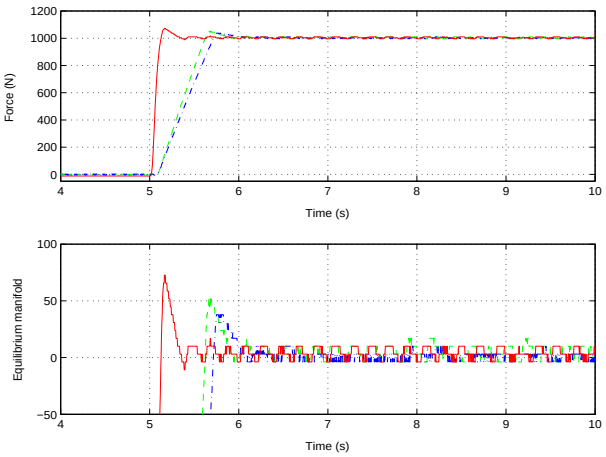

Fig. 2. Step force and equilibrium manifold responses using constant reaching law strategy for different gain constants (solid line : $K_\sigma = 5\times10^{-08}$, dash line : $K_\sigma = 4.5\times10^{-08}$, dash-dotted line : $K_\sigma = 4 \times 10^{-08}$)

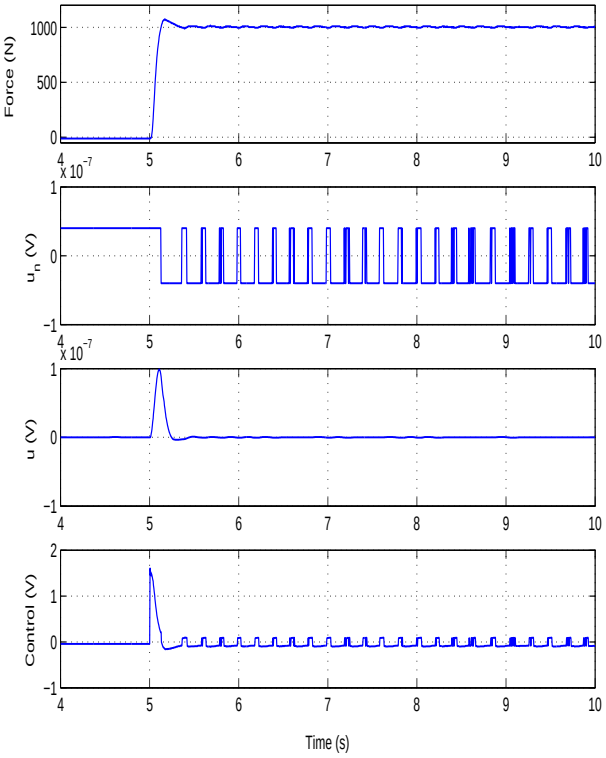

Fig. 3. Step force response and control components (u_n, u_c and u) for $K_\sigma = 5 \times 10^{-08}$

3.4.2. Constant plus Proportional Reaching Law To study the effect of VSC law with constant plus proportional reaching law, we added the proportional term $-K_p$ to the previous controller. Experiments were for $K_\sigma = 5\times10^{-08}$ and started at $t = 5s$ for $F_d = 1000N$. The controller parameters were selected to provide a similar force profile as in the previous test with reaching time $Tr \approx 0.5s$.
With reference to Fig. 4, by chosen constant plus proportional rate reaching law, the state is forced to approach the switching manifold faster when

$\sigma(\boldsymbol{x})$ is large. Our control leads to the satisfactory performance as shown in Fig. (4). In Fig. (5), we can see a major reduction in chattering of the control effort obtained by properly choosing of the parameter K_p. The reaching time is shorter than the results obtained with only a constant reaching law ($T_r = 1.2sec$) with the same overshoot and the control input is smooth. However, a small steady-state error($\approx 10N$) is observed.

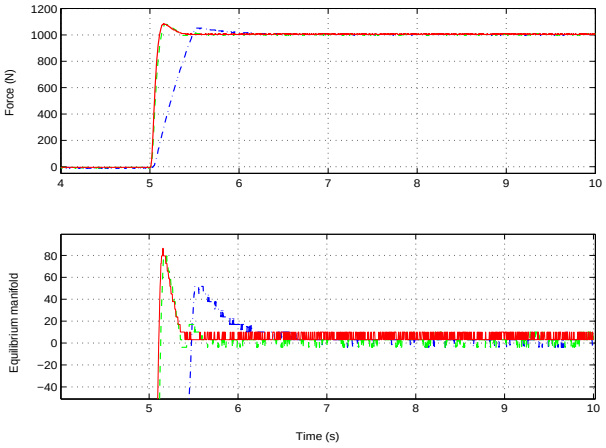

Fig. 4. Step force and equilibrium manifold responses using constant plus proportional reaching law strategy for different gain constants (solid line: $K_p = 0.02$, dash line: $K_p = 0.015$, dash-dotted line: $K_p = 0.001$)

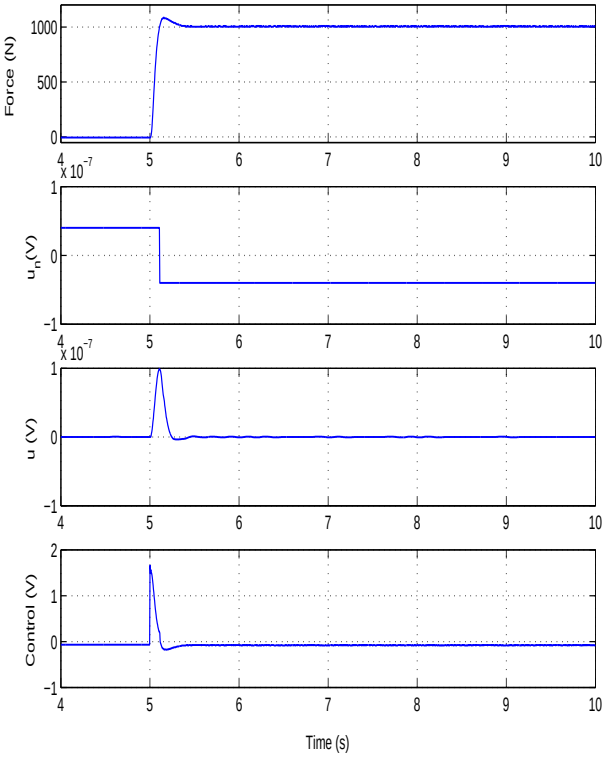

Fig. 5. Step force response and control components (u_n, u_c and u) for $K_p = 0.02$

3.4.3. Power Reaching Law The controller performances is now tested using the power reaching law strategy as described by equation (24). Experiments were done for $K_\sigma = 5 \times 10^{-08}$ and various values of α. Fig. 6 shows the responses of the hydraulic force F and the equilibrium manifolds ,$\sigma(\boldsymbol{x})$, are given for three values of gains α. With reference to Fig. (6), as α increases, the reaching time becomes smaller, but the chattering is severe and the overshoot is high. Chattering is reduced for $\alpha = 0.025$, but the reaching time is too long ($T_r \approx 1s$). This reaching law increases the reaching speed when the state is far away from the switching manifold, but reduces the rate when the state is near the manifold causing a long reaching time.
Fig. 7 shows the responses and the corresponding control components (u_n, u_c and u) for $\alpha = 0.25$ and $K_\sigma = 5 \times 10^{-08}$. We see a major reduction in the control effort, but regulating performance is poor and exhibits a severe chattering near the equilibrium manifold.

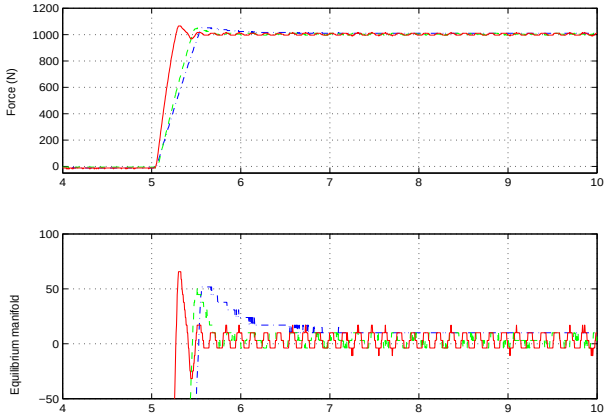

Fig. 6. Step force responses using power reaching law strategy for different gain constants (solid line: $\alpha = 0.25$, dash line: $\alpha = 0.075$, dash-dotted line : $\alpha = 0.025$)

3.4.4. Summary The controller parameters were chosen in order to provide, simultaneously, a good steady state and transient performance. From the above results one can see that using VSC with reaching law approach, the characteristics of the reaching mode can by controlled by a proper design of the reaching law equation (21). Making the parameter K_p large shortens the reaching time, but induce a large chattering. While making K_σ small reduces the chattering.

3.5 Conclusion

In this paper we presented the design, analysis, and experimental evaluation of a VSC law for an electro-hydraulic actuator using reaching law approach. The force controller was developed using sliding mode approach and it breaks down into two major phases. The first is the design of a nonlinear sliding mode manifold (surface) where the hydraulic system exhibits the desired properties in the presence of external disturbances. The second phase entails the development of a VSC law to drive the system to the equilibrium manifold. The dynamic of the equilibrium manifold was specified by three reaching law structure which affects the closed-loop performance (i.e., reaching

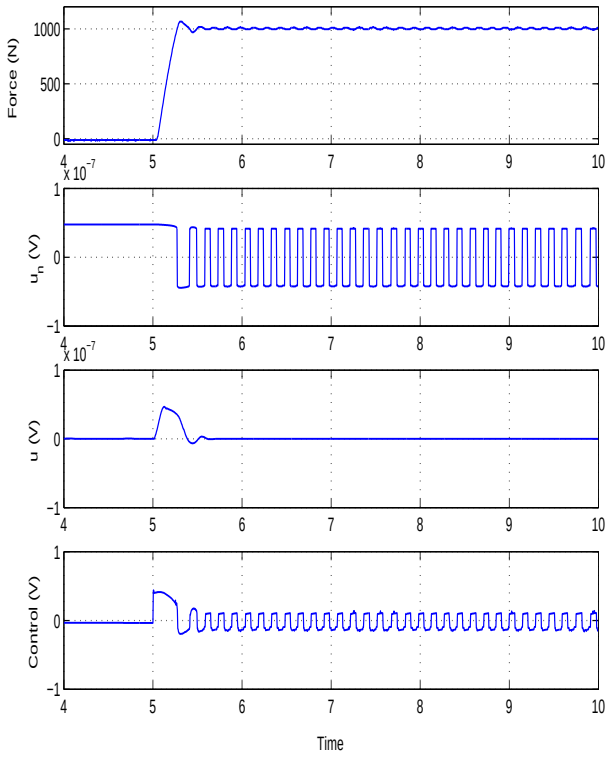

Fig. 7. Step force response and control components ($u_n, u_c, and \quad u$) for $\alpha = 0.25$ and $K_\sigma = 5 \times 10^{-08}$

time, chattering, overshoot, steady- state error). The proposed controllers were implemented on an fully equipped hydraulic test rig. A set of experimental tests were carried out and the effect of each strategy was analysed. The controller parameters were chosen in order to provide, simultaneously, a good steady-state and transient performance. From the experimental results one can see that the characteristics of the reaching mode can by controlled by a proper design of the reaching law equation. Experiments showed that all the controllers have the following advantages: Faster response, Low overshoot, Better steady state performance, and Chattering-free. A compromise is then necessary to achieve these goals.

In summary, the results of this work, which present a contribution to the application of VSC law in industrial applications, provide insights into the potential and the effectiveness of this technique for the stabilization of a hydraulic force control system. In particular, we have studied and compared the effect of three reaching law strategies on the hydraulic system performances.

REFERENCES

Alleyne, A., R. Liu, and H. Wright (n.d.). On the limitation of force tracking control for hydraulic active suspension. In: *American Control Conference*. Philadelphia, PA, USA. pp. 43–47.

Bobrow, J. E. and K. Lum (1995). Adaptive, high bandwidth control of a hydraulic actuator. In: *Proceedings of the American Control Conference*. pp. 71–75.

Gao, W. and C. J. Hung (1993). Variable structure control of nonlinear systems: A new approach. *IEEE Transaction Industrial Electronics* **40**(1), 45–55.

Huang, C. L., C. H. Lan and Y. C. Wu (1994). The position control of electrohydraulic servomechanism via a novel variable structure control. *Mechatronics* **4**(4), 369–391.

Jerouane, M. and F. Lamnabhi-Lagarrigue (2001). A new robust sliding mode controller for a hydraulic actuator. In: *40th IEEE Conference on Decision and Control*.

Kotzev, D. B., Cherchas and P. D. Lawrench (1994). Performance of generalized predictive control with on line model order determination for a hydraulic robotic manipulator. *Robotics* **13**, 55–64.

Lee, K. I and D. K. Lee (1990). Tracking control of a single road hydraulic cylinder using sliding mode. In: *29th SICE Annual Conference*.

Niksefat, N. and N. Sepehri (1999). Robust force controller design for a hydraulic actuator based on experimental input-output data. In: *American Control Conference*.

Niksefat, N. and N. Sepehri (2000). Design and experimental evaluation of a robust force controller for an electro-hydraulic actuator via quantitative feedback theory. *Control Enginnering Practice*.

Sohl, G. A. and J. E. Bobrow (1999). Experiments and simulations on the nonlinear control of a hydraulic servosystem. *IEEE Transaction Control System Technology* **7**(2), 238–247.